

Article

Electrochemistry-High Resolution Mass Spectrometry to Study Oxidation Products of Trimethoprim

Marc-André Lecours ¹, Emmanuel Eysseric ¹, Viviane Yargeau ², Jean Lessard ¹, Gessie M. Brisard ¹  and Pedro A. Segura ^{1,*} 

¹ Department of Chemistry, Université de Sherbrooke, Sherbrooke, QC J1K 2R1, Canada; marc-andre.lecours@usherbrooke.ca (M.-A.L.); Emmanuel.Eysseric@USherbrooke.ca (E.E.); Jean.Lessard@USherbrooke.ca (J.L.); Gessie.Brisard@USherbrooke.ca (G.M.B.)

² Department of Chemical Engineering, McGill University, Montreal, QC H3A 2B2, Canada; viviane.yargeau@mcgill.ca

* Correspondence: pa.segura@usherbrooke.ca; Tel.: +1-819-821-7922; Fax: +1-819-821-8019

Received: 26 November 2017; Accepted: 19 January 2018; Published: 24 January 2018

Abstract: The study of the fate of emerging organic contaminants (EOCs), especially the identification of transformation products, after water treatment or in the aquatic environment, is a topic of growing interest. In recent years, electrochemistry coupled to mass spectrometry has attracted a lot of attention as an alternative technique to investigate oxidation metabolites of organic compounds. The present study used different electrochemical approaches, such as cyclic voltammetry, electrolysis, electro-assisted Fenton reaction coupled offline to high resolution mass spectrometry and thin-layer flow cell coupled online to high resolution mass spectrometry, to study oxidation products of the anti-infective trimethoprim, a contaminant of emerging concern frequently reported in wastewaters and surface waters. Results showed that mono- and di-hydroxylated derivatives of trimethoprim were generated in electrochemically and possibly tri-hydroxylated derivatives as well. Those compounds have been previously reported as mammalian and bacterial metabolites as well as transformation products of advance oxidation processes applied to waters containing trimethoprim. Therefore, this study confirmed that electrochemical techniques are relevant not only to mimic specific biotransformation reactions of organic contaminants, as it has been suggested previously, but also to study the oxidation reactions of organic contaminants of interest in water treatment. The key role that redox reactions play in the environment make electrochemistry-high resolution mass spectrometry a sensitive and simple technique to improve our understanding of the fate of organic contaminants in the environment.

Keywords: redox reactions; EC-MS; Fenton reaction; fate of contaminants of emerging concern; transformation products

1. Introduction

In the late 1990s, researchers started to demonstrate the importance of investigating contaminants of emerging concern (EOCs) such as pharmaceuticals and personal care products and since then, the fate of these compounds in wastewater treatment plants and in the aquatic environment has been a topic of wide interest and active research. It is known that enzymes, such as those of the cytochrome P450 (CYP) super family, catalyze many oxidative reactions that transform EOCs during secondary (biological) water treatment processes or after these compounds are released into the natural environment [1]. The conventional method of the study of biotransformation products of organic contaminants involves extracting transformation products from in vivo experiments, or performing in vitro experiments using cellular extracts containing CYP450 enzymes [2,3]. In order to remove uninteresting compounds which might interfere with the analysis, reduce sample complexity and

simplify interpretation of the results, those approaches require laborious sample preparation to detect the compounds of interest [4]. In addition, performing experiments with biological systems requires the use of low concentrations of contaminants to avoid toxic effects leading to low concentrations of transformation products, making their identification and characterization even more difficult. Besides biological transformations, EOCs may be transformed after tertiary processes during wastewater treatment such as ozonation, ultraviolet light or advanced oxidation processes, i.e., chemical oxidation processes occurring via reactions with hydroxyl radicals [5]. Considering that these approaches do not generally result in complete mineralization under usual treatment conditions, these processes lead to the formation of unknown compounds [6,7]. To improve risk assessments for aquatic biota, it is important to understand the mechanisms of formation of those oxidation products as well as to elucidate their molecular structure [8].

Electrochemistry coupled offline or online with mass spectrometry is an interesting alternative to study oxidation products of EOCs, since experiments are done in controlled conditions using pure solvents and reagents and higher concentration of contaminants, reducing or eliminating the need for sample preparation and accelerating data analysis and identification workflows [9]. Mass spectrometry is well suited for coupling with electrochemistry given the rapidity, sensitivity and specificity of modern mass spectrometers. Studies have demonstrated that metabolites generated by enzyme-catalyzed reactions such as *N*-dealkylation, *N*-oxidation and *O*-dealkylation, aliphatic hydroxylation and aromatic hydroxylation can be generated *in vitro* by electrochemical methods [9,10]. The similarity between results obtained by such apparently unrelated systems (enzymatic vs. electrochemical cell) is explained by the underlying mechanisms that occur in the phase I metabolism, which are generally initiated by single electron transfer or hydrogen atom transfer involving an iron-oxygen complex [9,11]. For example, in electrochemical cells, single-electron transfer mechanisms such as the one occurring during *N*-dealkylation can be reproduced by oxidation reactions at the working electrode in the presence of a basic supporting electrolyte [11]. Electrochemistry was showed also to be useful to improve our understanding of abiotic processes that degrade or cause EOCs in the environment to bind to soils, as demonstrated by Hoffmann, et al. [12] with the sulfonamide antimicrobial sulfadiazine. It is clear at this point that electrochemistry cannot mimic all possible CYP450-catalyzed reactions, in fact only those reactions initiated by single-electron transfer (*N*-, *O*-, and *S*-dealkylation, hydroxylation of benzylic carbon, etc.) can be simulated by electrochemistry [13]. However, electrochemistry can be useful as a starting point to tackle the complexity found in samples issued from natural transformation processes, as it was demonstrated in a study on the transformation products of an EOC produced by the White-Rot Fungus *Pleurotus ostreatus* [14]. In that study, the formation of multiple complex biotransformation products of carbamazepine by electrochemistry, such as epoxy, dihydro and methoxy derivatives, was demonstrated using an online electrochemistry–mass spectrometry technique. According to the authors of that paper, workflows of identification of transformation products of organic contaminants can be improved by electrochemistry coupled to mass spectrometry.

The objective of the present work was to study the oxidation of a common EOC while demonstrating the usefulness of using electrochemistry coupled offline or online with mass spectrometry to improve our understanding of the fate of organic contaminants in the environment. Three different electrochemical experiments coupled offline to high-resolution mass spectrometry (HRMS) were investigated: cyclic voltammetry, electrolysis and the electro-assisted Fenton reaction. Also, an electrochemical experiment using a thin-layer flow cell coupled online to HRMS was performed. The anti-infective trimethoprim (TRI) was chosen as model compound given its frequent detection in environmental waters [15] and the availability in the literature of information on its oxidation products [16–21] and metabolites [22,23].

2. Material and Methods

2.1. Reagents and Chemicals

Trimethoprim was purchased from Santa-Cruz Biotechnology (Dallas, TX, USA). Tetrabutylammonium perchlorate (TBAP) was acquired from TCI America (Portland, OR, USA). 2,4-Diaminopyrimidine, 3,4,5-trimethoxytoluene, iron (II) sulfate and sodium sulfate were obtained from Sigma-Aldrich (St. Louis, MO, USA). All these products have a purity $\geq 98\%$. Water for electrochemistry experiments was purified using a Milli-Q filtration system (Merck Millipore, Burlington, MA, USA). Solvents and additives used in liquid chromatography–mass spectrometry experiments, such as acetonitrile (ACN), water and formic acid (FA), were purchased from Fisher Scientific (Ottawa, ON, Canada) and were Optima LC/MS grade.

2.2. Cyclic Voltammetry and Electrolysis

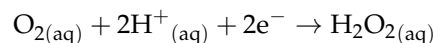
A three-compartment glass cell, each containing its own electrode, was used for both cyclic voltammetry (CV) and electrolysis experiments. The counter electrode, a Pt mesh connected to a Pt wire, was separated from the working electrode by a fine-sized glass frit. The reference electrode communicates with the central working compartment (volume ≈ 25 mL) via a Luggin capillary placed just below the surface of the working electrode. Working electrodes for cyclic voltammetry experiments had a 2 mm diameter and were made of glassy carbon, Au or Pt. For electrolysis experiments, the Au electrode was 6 mm and the glassy carbon 7 mm in diameter to improve the rate of transformation of TRI. The Ag/Ag⁺ reference electrode was prepared fresh on each day of the experiments. The reference solution consisted of 1 mL of ACN:H₂O 99:1 (*v/v*) solution with 100 mM (34.2 g·L⁻¹) TBAP as the supporting electrolyte to which 1 mM (169.9 mg·L⁻¹) AgNO₃ was added. An Ag wire was rubbed with fine sandpaper to remove the oxide layer and expose a fresh Ag surface. The wire was rinsed with ACN:H₂O 99:1 (*v/v*) before being immersed in the reference solution to form the reversible Ag/Ag⁺ redox couple. Organic medium such as ACN and TBAP is usually chosen to have access to a large potential window (very negative and very positive potential), this combination of solvent and salt is very stable in a wide range of potentials and various electrode materials. The presence of water (1% here) is added to furnish little and controlled amounts of protons.

To study the electrochemical behavior of TRI, CV experiments were used first to determine the general redox pattern of TRI and to monitor the potentials to be applied during subsequent electrolysis (constant potential) experiments. All experiments were performed at room temperature. Cyclic voltammetry experiments were carried out in a purely diffusional regime (working electrode was stationary) using conditions used in previous electrochemical oxidation studies [24,25]. Solutions of TRI (1 mM, 290.3 mg·L⁻¹) were prepared in ACN:H₂O 99:1 (*v/v*) with 100 mM TBAP. The supporting electrolyte was set at 100 mM to ensure a good conductivity of the solution. To eliminate reactions of radical intermediates with dissolved O₂, the working electrode compartment (anode compartment) was maintained under a N_{2(g)} atmosphere. N_{2(g)} was passed through a bubbler containing ACN to limit evaporation during prolonged experiments and the flow rate was adjusted to achieve moderate bubbling to limit undesirable convection phenomena. The cathode compartment was open to air. A CV of a blank solution of TBAP/ACN without TRI was always recorded before each experiment. The potential scan rate was set at 50 or 100 mV·s⁻¹ for all CV experiments.

Electrolysis experiments were done at constant potential and were conducted with a potentiostat/galvanostat EG&G model 273A from Princeton Applied Research. The solution was stirred to increase the supply of electroactive compound to the surface of the working electrode and to promote a higher conversion rate. Also, a higher concentration of TRI, 10 mM (2903 mg·L⁻¹) was used. After electrolysis, samples were diluted by a factor of 1000 using water and injected into the liquid chromatography–quadrupole–time of flight mass spectrometry (LC-QqTOFMS) system (Bruker, Billerica, MA, USA). This dilution step was necessary to avoid overloading the chromatographic column with the supporting electrolyte and to prevent signal saturation for the analyte.

2.3. Electro-Assisted Fenton Reaction

Electro-assisted Fenton reaction experiments were carried out with a potentiostat/galvanostat EG&G model 273A from Princeton Applied Research in a cell with one compartment and two electrodes. The working electrode was made of glassy carbon (diameter: 7 mm) and molecular oxygen is continuously bubbled into the solution during the experiment. In the electro-assisted Fenton reaction, hydrogen peroxide is generated in situ electrochemically in an acid medium from the dissolved oxygen:



Compared to other materials, glassy carbon shows a reduced overpotential with respect to the production of peroxide compared to other reactions, making it an ideal candidate [26] for this type of experiment. The hydroxyl radical (OH•) produced in the Fenton reaction reacts quickly with organic compounds in solution. For example, according to Dodd, et al. [27], the second order rate constant of the reaction of OH• with TRI is $(6.9 \pm 0.2) \times 10^9 \text{ M}\cdot\text{s}^{-1}$ at neutral pH and at 25 °C. When produced in sufficient quantity over a sufficient period of time, OH• will oxidize virtually all carbons in the molecule to lead to an almost complete mineralization of TRI. The counter electrode/reference electrode was a Pt mesh. The solution contained 50 mM Na₂SO₄, 0.1 mM FeSO₄ in water acidified to pH 2.7 using concentrated H₂SO₄. Since degradation of TRI in the electro-assisted reaction is fast, a higher concentration of TRI (58 mg·L⁻¹) was used in this experiment to follow changes in its concentration throughout the duration of the whole experiment. A current density of 1 mA·cm⁻² was applied for 30 min in galvanostatic mode. The reaction time and the current density were optimized to limit bubble formation at the counter electrode and to produce about 70% reduction of the signal of the precursor ion detected by mass spectrometry. Longer electrolysis time, e.g., >60 min, were not used to avoid further degradation of the transformation products which would then be harder to detect and characterize. All experiments were done at room temperature. Aliquots at different time intervals were sampled from the cell, diluted by a factor of 1000 and injected into the LC-QqTOFMS system.

2.4. Thin-Layer Flow Cell Coupled Online to High-Resolution Mass Spectrometry

The Roxy EC for MS System manufactured by Antec Leyden B.V. (Zoeterwoude, the Netherlands) was used to perform online EC-MS experiments. This system is composed of a syringe pump, a thin-layer flow cell (μ -PrepCell) and a three-electrode setup controlled by a potentiostat. The thin-layer flow cell has a 11 μ L internal volume. The reference electrode was Pd/H₂, the counter electrode was Ti and the working electrode was boron-doped diamond (dimensions 12 × 30 mm, thickness 1 mm). The cell was operated in the constant potential steps mode. All experiments were done at room temperature. The outlet of the thin-layer flow cell was connected to the inlet of the electrospray source of the QqTOFMS through a PEEK tubing (127 μ m internal diameter). TRI at a concentration of 4.3 μ M (1.25 mg L⁻¹) dissolved in a solution of 0.1% FA in H₂O:ACN 1:1 (pH 2.92) was introduced in the cell using a syringe pump at a flow rate of 20 μ L min⁻¹. This concentration was optimal to avoid saturating the QqTOFMS detector. The composition of the solution used for these experiments (0.1% FA in ACN:H₂O 1:1 *v/v*) was chosen according to manufacturer's recommendations [28].

2.5. Liquid Chromatography–Quadrupole–Time of Flight Mass Spectrometry (LC-QqTOFMS)

Chromatographic separation of electrolysis or Fenton reaction products was performed on a Nexera ultra performance liquid chromatograph (UPLC) manufactured by Shimadzu (Kyoto, Japan) coupled to a Bruker MaXis time-of-flight mass spectrometer (QqTOFMS) equipped with an electrospray ionization (ESI) source operated in the positive mode. Reaction products generated in the thin-layer flow cell were not separated chromatographically since the cell is coupled online to the QqTOFMS and reaction products are monitored in real time.

The UPLC parameters were the following: the column was an Acquity HSS-T3 C₁₈ reverse phase (50 × 2.1 mm, 1.8 μm), the mobile phase was composed of solvent A (0.1% FA in H₂O) and solvent B (0.1% FA in ACN) and the mobile phase flow rate was 500 μL·min⁻¹. The elution gradient was adjusted according to the samples to maximize separation. Therefore, two different gradients were employed for optimal separation: one for electrolysis products and the another for electro-assisted Fenton reaction products. For the analysis of electrolysis products, the gradient as percentage of B in the mobile phase was: at 0 min, 10%; 5.30 min, 15%; 7 min, 40%; 9 min, 98%; 10 min, 98%; 11 min, 10%; 14 min, 10%. For the analysis of Fenton reaction products, the gradient used was the following: 0 min, 5%; 5 min, 20%; 7 min, 50%; 8 min, 98%; 10 min, 98%; 11 min, 5%; 14 min, 98%. For both chromatographic methods the column temperature was set to 30 °C.

The injection volume was also adjusted according to the experiment and the sample. Thus between 0.1 and 2 μL of the diluted sample was injected to obtain a signal with a target intensity of 2 × 10⁵ for the most abundant species. A switching valve was used to bypass supporting electrolyte (TBAP) which remains sufficiently concentrated to saturate the QqTOFMS detector.

The QqTOFMS parameters were the following: nebulizing gas N₂, nebulizing gas temperature 200 °C, nebulizing gas flow rate 9 L·min⁻¹, capillary voltage 3500 V, end plate offset -500 V, ion cooler 35 μs and RF 55 Vpp. The mass range was *m/z* 100 to 700. For the MS/MS experiments, a time segment comprising the peak of the analyte was created and the isolation window of the precursor ion was set to 1 Da. The collision energies (between 10 and 30 eV) were optimized to obtain 10% relative intensity of the precursor ion. The mass resolution measured at full width at half-maximum for *m/z* 291 was about 18,000.

2.6. Identification of Oxidation Products

To identify the oxidation products generated in the diverse electrochemical setups, a workflow based on the confidence level scheme proposed by Schymanski et al. [29] was adopted. According to that scheme, accurate mass represents the lowest confidence (level 5), followed by unequivocal molecular formula (level 4), tentative candidate (level 3, based on complementary data such as tandem mass spectra and software tools), probable structure (level 2a, reached using a library spectrum match or level 2b reached using experiments indicating that no other structure fits the data) and finally confirmed structure (level 1, which requires a reference standard). Since tandem mass (MS/MS) spectra of oxidation products of trimethoprim are not yet stored in spectral libraries and standards are rare or not commercially available, diverse techniques were used to improve the identification level of the accurate mass data obtained by the high-resolution mass spectrometer. Those complementary techniques were: hydrogen–deuterium exchange (HDX) [30], which reveals the number of exchangeable hydrogen atoms such as those present in alcohol or amine functional groups; MS/MS experiments and comparison with MS/MS data found in the literature; in-silico fragmentation analysis of precursor ions based on the Mass Frontier software from HighChem and spectral accuracy determined by MassWorks software from Cerno Bioscience. Spectral accuracy measures the similarity between mathematically transformed experimental isotopic pattern of an ion and the theoretical isotopic pattern corresponding to a given molecular formula [31]. High spectral accuracy, generally ≥98%, means that the experimental isotopic pattern closely matches the abundance and shape of the isotopic pattern expected for a possible formula. Therefore, spectral accuracy contributes to eliminate possible candidates and gives higher confidence in the assignation of unique molecular formulas to accurate masses. Parameters for spectral accuracy were the following: elements (C, H, N and O); number of elements determined by empirical rules, mass tolerance (10 Da); charge (+1) and number of double bond equivalents (3.5 to 11.5).

Parameters for the in-silico fragmentation analysis using Mass Frontier software were the following: ionization method (M + H⁺); ionization on non-bonding electrons and π-bonds; cleavage (α and inductive); H-rearrangement (charge remote rearrangement, hydrogen transfer from atom α, β and γ); resonance reaction (electron sharing, charge stabilization); aromatic system allowed

(ionization, stabilization); cleavage allowed on primary, secondary and tertiary carbocation; maximum reaction steps (5) and reactions limit (10).

3. Results and Discussion

3.1. Cyclic Voltammetry and Electrolysis

The results of CV measurements with TRI are shown in Figure 1. They revealed two main peaks in the voltammogram at 900 and 1150 mV (vs. Ag/Ag⁺). Those peaks indicate the oxidation of two electroactive functions on the TRI molecule and the formation of two oxidation products at the electrode surface. Electrolysis experiments based on those two potentials were performed to produce a sufficient quantity of oxidation products for identification by offline LC-QqTOFMS. Minor peaks were also observed at negative potentials which may have been the result of an incomplete purge of O₂ by N₂ bubbling. Nevertheless, the presence of possible traces of O₂ did not influence TRI oxidation.

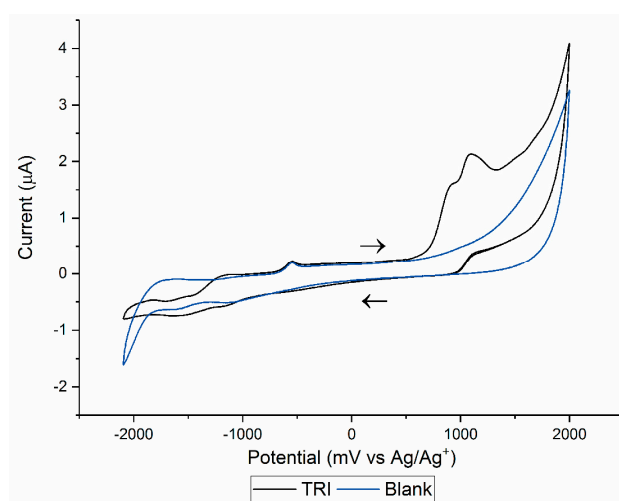


Figure 1. Cyclic voltammogram of trimethoprim (TRI) in the three-compartment electrochemical cell using a glassy carbon working electrode (2 mm of diameter) and a solution of ACN:H₂O 99:1 and 100 mM tetrabutylammonium perchlorate (TBAP). Potential scan rate was 50 mV s⁻¹. Arrows indicate the signal corresponding to the forward and reverse scans.

Electrolysis experiments were initially performed at a constant potential of 1050 mV, i.e., at a potential between the two oxidation peaks observed in the cyclic voltammetry experiments. The solution was stirred to maximize the supply of reagent to the surface of the electrode. During these experiments, a layer of precipitate formed on the surface of the working electrode regardless of the material used, Au or Pt. That solid product accumulated until small flakes started to detach and settle at the bottom of the cell. At the end of the electrolysis, the solution was diluted by a factor of 1000 in water and analyzed by LC-QqTOFMS. Results did not show the presence of any reaction product. To investigate the nature of the layer formed on the electrode, the cell was placed in a sonicator for 1 min to detach the precipitate from the glass wall and facilitate its recovery by dissolving it in methanol. Analysis of that methanol solution by LC-QqTOFMS showed only the presence of TRI. The presence of TRI in that solution was most likely the result of a contamination, i.e., TRI was adsorbed on the layer of precipitate.

When the potential applied during the electrolysis was increased to 1500 mV, i.e., after the second oxidation peak of TRI, and after 60 min of electrolysis, the solution acquired a slightly beige tint and no layer was formed on the surface of the electrode, thus suggesting the formation of soluble oxidation products, and a sample of the solution was collected. The sample was diluted by a factor of 1000 in water and injected in the LC-QqTOFMS. Results showed the presence of an oxidation

product having an ion of m/z 307.1411 which was named oxidation product 306 or OP306 because its molecular mass is 306 Da. Analysis of spectral accuracy of the isotopic pattern in MassWorks indicated that only two neutral formulas were possible for that ion considering the constraints specified in the Material and methods section: $C_{14}H_{18}N_4O_4$ ($\Delta m = 1$ mDa, spectral accuracy = 93.9%) and $C_9H_{10}N_6O_6$ ($\Delta m = 5$ mDa, spectral accuracy = 92.2%). Since the number of N atoms in the oxidation should not be higher than in TRI and considering that the spectral accuracy for the first formula was higher, the unequivocal molecular formula was determined to be $C_{14}H_{18}N_4O_4$. This formula indicated the addition of one O atom relative to TRI ($C_{14}H_{18}N_4O_3$) in OP306. HDX experiments using a technique recently developed in our group [32] indicated an increase of one exchangeable H atom in OP306 (total of five exchangeable H atoms) relative to TRI (four exchangeable H atoms). MS/MS experiments with OP306 using a collision energy of 30 eV gave the product ions shown in Table 1. Transformation products of TRI with the same molecular formula, number of exchangeable hydrogens, precursor ion and product ions (Table 1) have been previously reported by several authors and were produced by rat metabolism [32], pig liver microsomes [33] and diverse water treatment processes [16,18,19,22]. Proposed structures are shown in Figure 2 (isomers A, B and C).

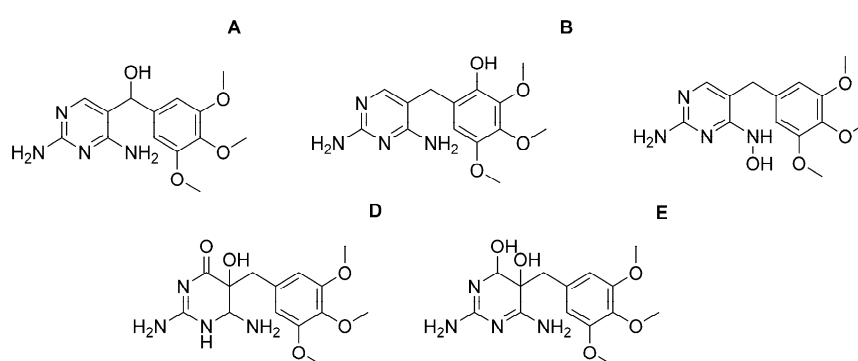


Figure 2. Tentative molecular structures for TRI transformation products according to previous studies. (A–C): Proposed structures for OP306. (D,E): Proposed structures for OP324.

From isomers A, B and C shown in Figure 2, OP306 appears to correspond to α -hydroxytrimethoprim (α -OH-TRI, isomer A) since it is the best match to MS/MS data. Two reaction mechanisms, based on single-electron transfer and nucleophilic attack by H_2O , are proposed to explain the electrochemical formation of OP306 (Figure 3 and Figure S1, Supplementary material). A hypothesis explaining the difference between the electrolysis products observed at 1050 and 1500 V is illustrated in Figure 3. The first step in the electrolysis of TRI, is the loss of an electron which generates a radical intermediate. This radical intermediate can react with TRI to form dimers or other TRI oligomers. At higher potentials, further oxidation (followed by the loss of a proton) of the radical intermediate is possible, thus resulting in a second cationic intermediate that cannot be further oxidized and that ultimately leads to the formation of α -OH-TRI after the loss of a proton and nucleophilic attack by water.

The formation of α -OH-TRI by electrochemistry in the electrolysis experiments was selective as is shown in Figure S2 (Supplementary material). No other major oxidation product between m/z 200 and 400 was observed in the chromatograms after 7 min of analysis (TRI eluted at around 6 min). While it is possible that dimers or other TRI dimers or oligomers could have been formed in the electrolysis at 1500 V, they do not appear to be major products. Also, detection of such species in the conditions used could be difficult since they would have eluted by the end of the chromatographic gradient. In those conditions, many column contaminants are eluted given the high organic content in the mobile phase. Those compounds can cause signal suppression, thus avoiding detection of minor sample components.

Table 1. Proposed molecular formulas and major product ions of the precursor ions observed in the electrochemistry experiments.

Observed Ions (<i>m/z</i>)	Name	Most Likely Molecular Formula ^a (Neutral)	Δm (mDa)	Spectral Accuracy (%)	RDBE ^b	Product Ions ^c (<i>m/z</i>)
Electrolysis						
307.1411	OP306	C ₁₄ H ₁₈ N ₄ O ₄	1	93.9	7.5	259.0825 (100), 243.0875 (58), 274.1055 (22), 289.1286 (11)
Electro-assisted Fenton reaction						
237.1026	OP236	C ₁₀ H ₁₂ N ₄ O ₃	4	64.6	6.5	N.A.
		C ₁₃ H ₁₆ O ₄	−10	64.8	5.5	
291.1082	OP290	C ₁₃ H ₁₄ N ₄ O ₄	0.5	N.A.	8.5	258.0736 (100), 273.0984 (66), 240.0645 (44), 241.0703 (40), 291.1084 (31)
307.1398	OP306	C ₁₄ H ₁₈ N ₄ O ₄	−0.2	69.8	7.5	259.0822 (100), 243.0878 (60), 274.1054 (30), 231.0869 (14), 244.0927 (14)
323.1345	OP322a	C ₁₄ H ₁₈ N ₄ O ₅	−0.5	89.2	7.5	249.0983 (100), 231.0887 (88), 259.0827 (86), 216.0624 (73), 323.1345 (59)
323.1346	OP322b	C ₁₄ H ₁₈ N ₄ O ₅	−0.4	84.6	7.5	249.0979 (100), 231.0875 (90), 259.0826 (78), 216.0637 (45), 323.1349 (41)
325.1504	OP324	C ₁₄ H ₂₀ N ₄ O ₅	−0.2	87.3	6.5	181.0680 (100), 325.1497 (55)
Thin later flow cell coupled online to high-resolution mass spectrometry (HRMS)^d						
307.1421	OP306	C ₁₄ H ₁₈ N ₄ O ₄	2	50.3	7.5	N.A.
323.1372	OP322	C ₁₄ H ₁₈ N ₄ O ₅	2	92.9	7.5	323.1372 (100), 259.0998 (22), 291.1109 (20), 231.0893 (13)
339.1325	OP338	C ₁₄ H ₁₈ N ₄ O ₆	3	N.A.	7.5	N.A.
357.1431	OP356	C ₁₄ H ₂₀ N ₄ O ₇	3	N.A.	6.5	N.A.
398.1700	OP397	C ₁₀ H ₂₃ N ₉ O ₈ *	−4	94.1	3.5	N.A.
		C ₁₁ H ₂₃ N ₇ O ₉ *	7	94.1	3.5	
		C ₁₆ H ₂₃ N ₅ O ₇ *	3	92.0	7.5	

^a According to mass accuracy (tolerance = 10 mDa), spectral accuracy and number of C and N atoms in the candidate structures (candidates with number of C and N atoms higher than those of trimethoprim (TRI) were eliminated). ^b Ring and double bond equivalents. ^c Values between parentheses indicate normalized abundance at a collision energy of 30 eV. ^d Values between parentheses indicate normalized abundance at a collision energy of 20 eV. * Indicates that no possible candidate formula was possible within the constraints given, therefore a higher number of C and N atoms relative to TRI was allowed to determine a molecular formula. N.A.: Not available.

The TRI oxidation product α -OH-TRI has been observed in living systems such as rat metabolism [32], and biological and chemical process like nitrifying bacteria in activated sludge [22], direct photolysis and solar TiO_2 photocatalysis [16], oxidation by KMnO_4 [18] and thermo-activated persulfate oxidation [19]. This demonstrates the diversity of phenomena in which electrochemistry can play an important role in predicting, identifying and understanding the formation of transformation products of EOCs generated by diverse and dissimilar systems involving redox reactions.

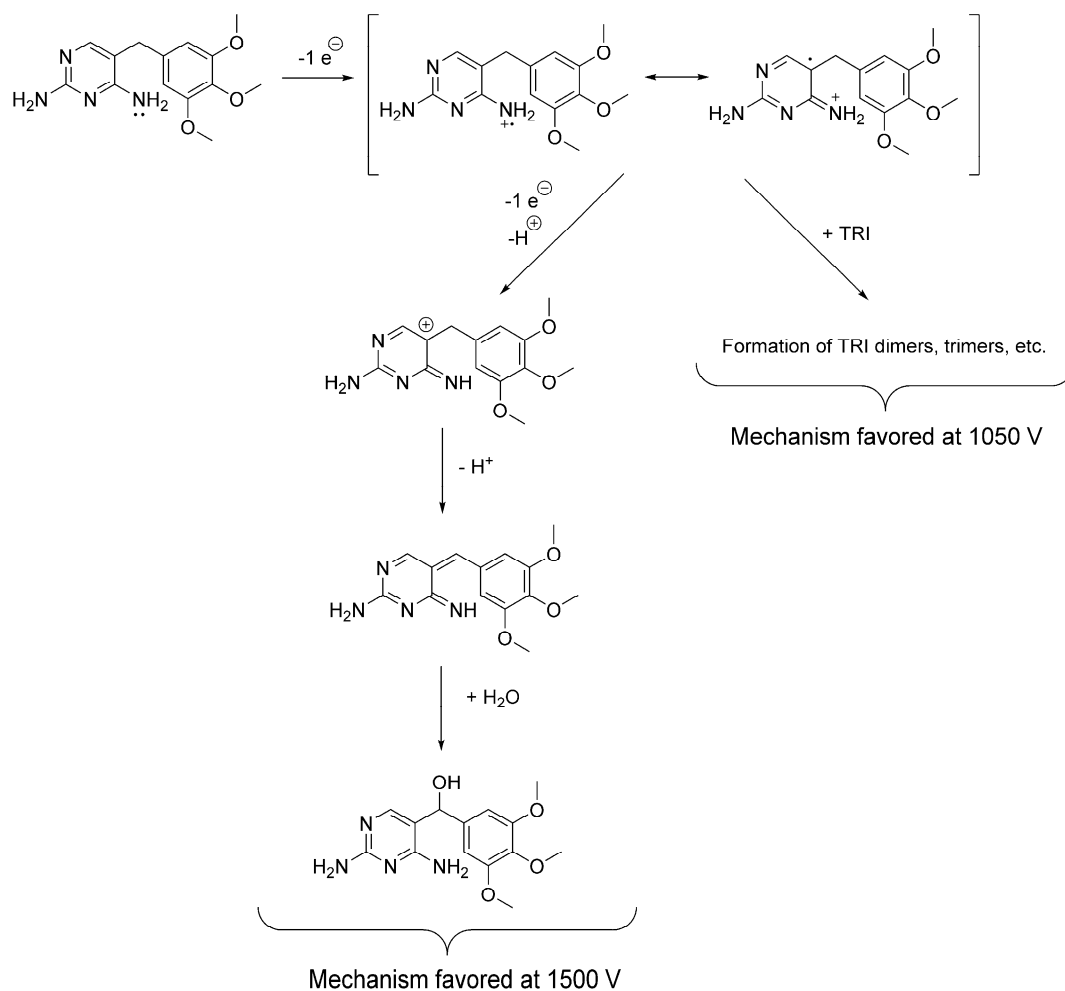


Figure 3. Proposed mechanism of formation of α -OH-TRI by electrolysis at 1500 V. The formation of the unidentified precipitated at 1050 V could be explained by the reaction of a radical intermediate with TRI.

3.2. Electrochemically-Assisted Fenton Reaction

These experiments showed that after 60 min of reaction, TRI was completely transformed (Figure 4). Several major transformation products with ions of m/z 237, 291, 307, 323 and 325 were formed during the experiment and they reached their maximum concentration between 10 to 20 min of treatment. After this maximum, the transformation products were also degraded and were no longer detected after 60 min of treatment, except for one transformation product which appeared to be resistant to degradation, the oxidation product with a m/z of 237.

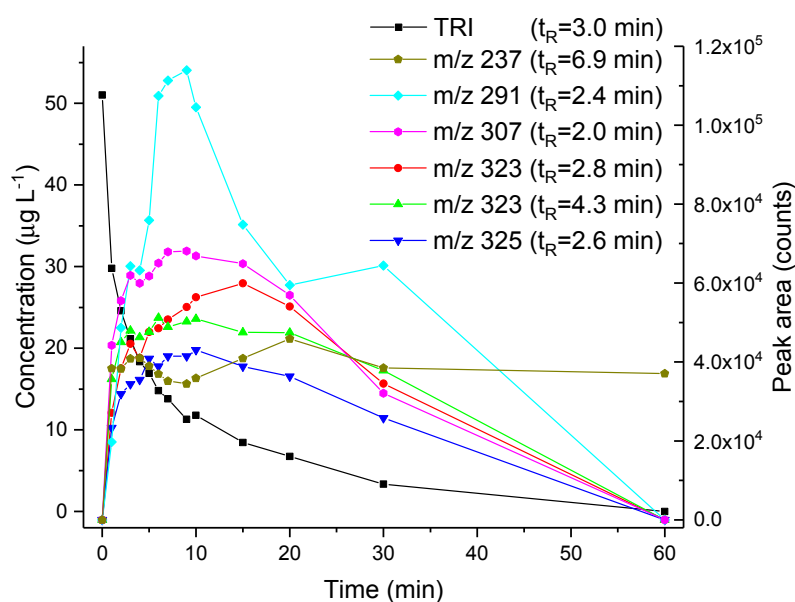


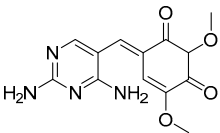
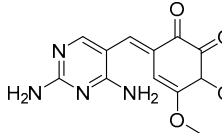
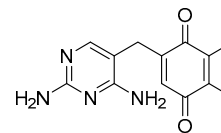
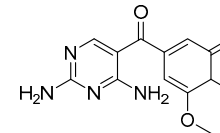
Figure 4. Profile of degradation of TRI and formation of its transformation products with the electro-assisted Fenton reaction setup. Only the concentration of TRI was measured (left axis). For the oxidation products, peak areas were used to measure their relative abundance as a function of time (right axis).

To the authors' knowledge, OP236 (m/z 237.1026) has not been reported previously in the literature. For this compound (Table 1), only two candidates were possible: $C_{10}H_{12}N_4O_3$ ($\Delta m = 4$ mDa, spectral accuracy = 64.6%), and $C_{13}H_{16}O_4$ ($\Delta m = -10$ mDa, spectral accuracy = 64.8%). Unfortunately, it was not possible to perform MS/MS experiments since precursor abundance was too low and further experiments are necessary to unambiguously assign its molecular formula.

As for m/z 291.1083 (OP290), formula determination based on mass and spectral accuracy suggested that one two molecular formulas are possible candidates: $C_{13}H_{14}N_4O_4$ ($\Delta m = -0.5$ mDa, spectral accuracy = 74.1%) or $C_{12}H_{18}O_8$ ($\Delta m = 0.9$ mDa, spectral accuracy = 74.1%). From those two, $C_{13}H_{14}N_4O_4$ is obviously the most probable candidate since it is extremely unlikely that TRI could have lost four N atoms while retaining 12 C atoms (loss of two C atoms) and accepted four additional O atoms upon its oxidation. Five potential structures corresponding to the formula $C_{13}H_{14}N_4O_4$ were suggested, as presented in Table 2. An in-silico MS/MS fragmentation analysis based on theoretical and library reactions on MassFrontier software showed that only one among those five structures (isomer E) could explain 10 of the 12 most abundant product ions of m/z 291.1083, with mass accuracy for all matching fragments ≤ 2.5 mDa.

In a previous study of the transformation of TRI under aerobic conditions in nitrifying activated sludge, this same structure was assigned to a transformation product of TRI with the same exact mass, albeit a completely different MS/MS spectrum [34]. While differences in MS/MS could be the result of different mass analyzers (the present study used an QqTOF while in the study of Jewell et al. a linear ion trap-orbitrap mass spectrometer was used) mass accuracy, spectral accuracy and comparison of MS/MS spectrum and in silico fragmentation suggests that the most likely structure of OP290 is isomer E or (2,4-diaminopyrimidin-5-yl)-(4-hydroxy-3,5-dimethoxyphenyl)methanone.

Table 2. Mass accuracy of the product ions of the five proposed structures for OP290 according to in-silico fragmentation analysis done by Mass Frontier software.

Observed Product Ions <i>m/z</i>	Relative Abundance %	Isomer				
		A	B	C	D	E
						
212.0700	10.5					−0.7
216.0519	14.3					
230.0790	18.3					0.8
234.0660	9.4					−2.5
240.0645	43.9					
241.0703	40.4		1.7			1.7
249.0866	25.4	11.6	0.4	0.4	11.6	0.4
258.0736	100	13.7	1.1	1.1	1.1	1.1
261.0613	8.0					0.5
261.0968	6.5	1.4	1.4	1.4	1.4	1.4
273.0984	66.4	−0.2	−0.2	−0.2	−0.2	−0.2
276.0849	15.0	13.0	13.0	13.0	13.0	0.4

Note: A few ions were omitted from this table if the accurate mass and the abundance were close to the expected $M + 1$ isotopic peaks.

Chromatograms showed that the oxidation product with a retention time of 2.0 min had an ion of m/z 307.1398 and eluted earlier than TRI on the C_{18} column, similar to OP306 (α -OH-TRI), the oxidation product observed in the electrolysis experiments with the three-compartment cell with stationary electrodes. Mass accuracy (-0.2 mDa) and spectral accuracy (69.8%) also suggested that the most likely neutral formula for that compound is $C_{14}H_{18}N_4O_4$ since the other two possible candidates ($C_{16}H_{14}N_6O$, $C_9H_{18}N_6O_6$) had a higher number of N atoms relative to TRI, which is not possible in this reactive system. The low spectral accuracy of the most likely candidate was due to the low signal-to-noise ratio signal, and the presence of background peaks interfering with the determination of spectral accuracy. Peaks in the MS/MS spectrum of m/z 307.1398 (Table 1) showed that product ions generated after collision induced dissociation (m/z 243, m/z 244, m/z 259 are m/z 274) are the same as those of OP306 observed in the three-compartment electrode cell with stationary electrodes (Table 1). This suggests that α -OH-TRI can also be formed in the electro-assisted Fenton reaction setup.

The presence of two oxidation products of m/z 323, OP322a eluting at 2.8 min, and the other, OP322b, with a retention time of 4.3 min was also observed. Spectral accuracies (89.2% and 84.6%, respectively) and mass accuracies (-0.5 and -0.4 mDa, respectively) unambiguously indicated that the neutral formula of both OP322a and OP322b was $C_{14}H_{18}N_4O_5$. MS/MS experiments revealed that those two isomers share the same major product ions: m/z 249, m/z 231, m/z 259, m/z 216 and m/z 232 (Table 1). Therefore, they must have a very similar structure. For example, the addition of oxygen must have occurred at close positions on the OP322a and OP322b molecule, such as on the ring of the 3,4,5-trimethoxyphenyl moiety or on the amine groups to yield *N*-oxides. However, those oxygen additions decreased the retention of OP322a more significantly than that of OP322b, since the difference of retention time between the two isomers is of 1.5 min. Oxidation products of TRI with the same molecular formula have been reported earlier by several authors working on advanced oxidation processes for water treatment and these were identified as dihydroxy-TRI isomers [16,19]. At least five isomers of OP322 were reported by Sirtori, et al. [16]. In another study, two other isomers were proposed for OP322 and were explained by cleavage of the 2,4-diaminopyrimidinyl moiety but the MS/MS spectrum reported by the authors in that study [18] had only one product ion (m/z 181) which does not correspond the one observed experimentally in the present study (Table 1).

Another oxidation product observed was m/z 325.1504 (OP324). Spectral accuracy (87.3%) and mass accuracy (-0.2 mDa) pointed to $C_{14}H_{20}N_4O_5$ as the most likely molecular formula and the other possible candidates (e.g., $C_{20}H_{20}O_4$ or $C_{16}H_{16}N_6O_2$) had a higher number of C or N atoms relative to TRI. A compound with the same molecular formula (compound D, Figure 2) was also identified in TRI degradation experiments with sludge containing nitrifying bacteria [22]. The only product ion of m/z 325.1504 observed by MS/MS, m/z 181 (Table 1), is also the only product ion reported by Eichhorn et al. [22]. Another study on the oxidation of antibiotics during water treatment with $KMnO_4$ [18] suggested a different molecular structure for a TRI oxidation product of formula $C_{14}H_{20}N_4O_5$ and similar MS/MS spectrum. Such structure (Figure 2, compound E) is also possible. Unfortunately, HDX combined with MS/MS experiments were not performed on OP324, which could have helped determine the correct structure since some exchangeable hydrogens in both compounds are located in different parts of their structure.

Contrary to the CV and electrolysis experiments, in the electro-assisted Fenton reaction there was no interaction between TRI and the surface of the electrode. The reactions leading to these transformation products take place within the solution. Besides being able to mimic certain reactions resulting from the metabolism of cytochrome P450 enzymes, as reported earlier [10], the electro-assisted Fenton reaction is an interesting approach to study oxidation reactions occurring during water treatment processes involving $OH\bullet$.

3.3. Thin-Layer Flow Cell Coupled Online to High-Resolution Mass Spectrometry

One of the major advantages of the thin-layer flow cell compared to the other setups used is the possibility of online coupling with a mass spectrometer. Such a setup allows us to detect in real time

compounds formed in the cell when a potential is applied. This setup saves enormous amounts of time but it also comes with certain limitations: (i) the solution composition must be compatible with electrospray ionization, i.e., the supporting electrolyte must be kept at low concentration, usually around 0.1% *v/v* or ≤ 50 mM; (ii) the supporting electrolyte must be volatile, such as FA or ammonium formate; and (iii) there is no chromatographic data, reaction products are introduced directly into the mass spectrometer, therefore isomers cannot be resolved.

Figure 5 shows the results of experiments performed using constant potential steps with a solution containing TRI at $1.25 \text{ mg}\cdot\text{L}^{-1}$. Preliminary experiments showed that no reaction product was observed below 750 mV (vs. H_2/Pd) using the boron-doped diamond (BDD) working electrode. Reaction products started to be detectable at +1000 mV and a progressive diminution of the TRI ion (m/z 291) was observed when increasing the potential. At +2500 mV, the signal of TRI was about 0.5% of its original value when the cell was off.

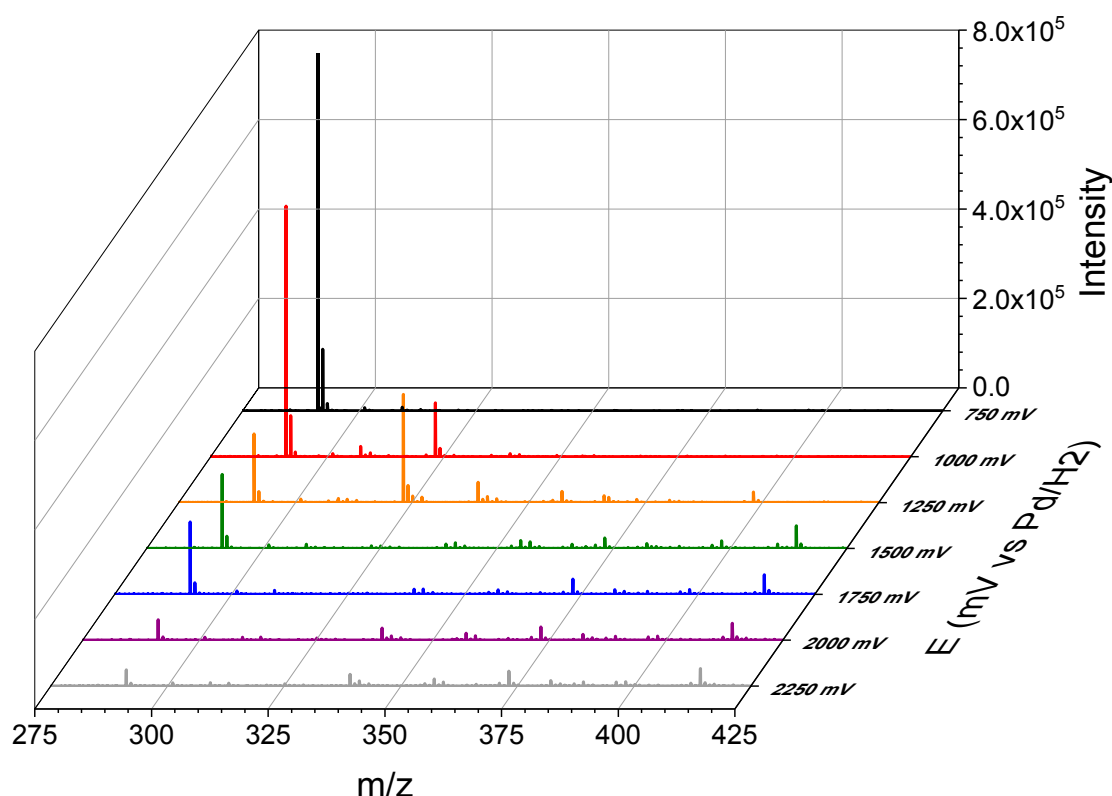


Figure 5. Mass spectrometry voltammogram of TRI obtained with the thin-layer flow cell coupled online with the QqTOFMS. The solution was composed of 0.1% FA in ACN:H₂O 1:1 and the concentration of TRI (m/z 291) was $1.25 \text{ mg}\cdot\text{L}^{-1}$.

The most abundant oxidation products were detected between +1000 and +1250 mV and are reported in Table 1. Amongst that list, the most intense signal corresponded to m/z 323.1372 ($\text{C}_{14}\text{H}_{18}\text{N}_4\text{O}_5$, $\Delta m = 2$ mDa, spectral accuracy = 92.9%) and it was observed at both 1000 and 1250 mV (vs. Pd/H_2). Tandem mass (MS/MS) spectra experiments (Table 1) confirmed that $\text{C}_{14}\text{H}_{18}\text{N}_4\text{O}_5$ (or most likely a mixture of compounds of molecular formula $\text{C}_{14}\text{H}_{18}\text{N}_4\text{O}_5$) generated in the thin-layer flow cell are the same as the dihydroxy-TRI isomers (OP322a and OP322b) observed in the Electro-assisted Fenton reaction experiments. Also, m/z 307.1421 ($\text{C}_{14}\text{H}_{18}\text{N}_4\text{O}_4$, $\Delta m = 2$ mDa, spectral accuracy = 50.3%) observed only at 1000 mV (vs. H_2 -Pd) and m/z 339.1325 ($\text{C}_{14}\text{H}_{18}\text{N}_4\text{O}_6$, $\Delta m = 2$ mDa) observed at 1250 mV (vs. H_2/Pd) were observed and appear to be mono and trihydroxylated-TRI, respectively. As for m/z 357.1431 (1250 mV vs. H_2/Pd), it could correspond to $\text{C}_{14}\text{H}_{20}\text{N}_4\text{O}_7$ ($\Delta m = 3$ mDa). However, unequivocal molecular formulas for this ion cannot be confirmed since

the relative low abundance and signal-to-noise ratio of these compounds resulted in low spectral accuracy or isotope patterns that did not correspond to the proposed formulas, as was the case of m/z 339.1325 (1250 mV vs. H_2/Pd). Also, meaningful MS/MS spectra could not be obtained because of the low signal of these two ions. However, the presence of multiple hydroxylated oxidation products of TRI in the thin-layer flow cell is highly possible. Multiple hydroxylated species of nucleotides have been observed when using a similar setup with the same electrode, albeit at both higher pH and potential [35]. Electron transfer from TRI to the electrode surface may not be the only mechanism responsible for the formation of TRI oxidation products in the BDD electrode; $OH\bullet$ radicals most probably intervened in their formation as well. Indeed, Marselli, et al. [36] have shown that $OH\bullet$ radicals are formed in the oxidation of water on a BDD electrode. A previous study on the degradation of TRI in a photoelectro-Fenton process also reported the formation of multiple hydroxylated oxidation products of TRI [37].

The presence of m/z 398.1700 (1250 mV vs. H_2/Pd), is however puzzling since no molecular formula with a number of C and N atoms equal or lower than those in TRI can be assigned to this ion. Therefore, this ion may correspond to an addition or condensation reaction product between TRI oxidation products. Such reactions are not unlikely, since the generation of radical species by electrochemistry often leads to oligomerization or polymerisation reactions [38]. Studies on the oxidation of the skin allergen *p*-phenylenediamine using a thin-layer flow cell with a BDD working electrode showed that ions corresponding to *p*-phenylenediamine dimers were formed [39]. The nature of such reactions products was not investigated here and were considered out of the scope of the present study.

Results obtained with this setup showed that coupling a thin-layer flow cell with a BDD electrode to a high-resolution mass spectrometer provides an interesting tool for studying the oxidation products of organic compounds in the environment and water treatment process involving $OH\bullet$ such as photolysis and advanced oxidation processes. In this setup, the effect of potential on the formation of oxidation products can be monitored in real time, which allows a more efficient interpretation of data.

In summary, the diverse electrochemical approaches used in the present study showed that mostly mono-, di-hydroxylated and possibly tri-hydroxylated derivatives of trimethoprim were generated electrochemically (Table 3). Those compounds have been previously reported as mammalian [32] and bacterial metabolites [22] as well as transformation products of advanced oxidation processes applied to waters containing trimethoprim [16,18,19,37]. These results suggest that electrochemistry–high resolution mass spectrometry is an interesting technique for studying oxidative reactions of organic compounds of environmental interest, as was previously suggested by Hoffmann et al. [12].

Table 3. Summary of techniques tested and the main results obtained.

Technique	Conditions	TRI Oxidation Products Generated	Identification Level [29]	Previous Reports of the Oxidation Product
Electrolysis	<i>Solution:</i> ACN:H ₂ O 99: 1 (<i>v/v</i>) with 100 mM TBAP. <i>WE:</i> Glassy carbon maintained under a N _{2(g)} atmosphere. <i>Potential applied:</i> 1500 mV (vs. Ag/Ag ⁺).	OP306 (α -OH-TRI)	Probable structure (level 2b): based on spectral and mass accuracy, H/D exchange, experimental and literature MS/MS spectra.	Rat metabolism [32]. Nitrifying bacteria in activated sludge [22], direct photolysis and solar TiO ₂ photocatalysis [16], Oxidation by KMnO ₄ [18], thermo-activated persulfate oxidation [19].
Electro-assisted Fenton reaction	<i>Solution:</i> 50 mM Na ₂ SO ₄ , 0.1 mM FeSO ₄ in acidified H ₂ O with H ₂ SO ₄ at pH 2. <i>WE:</i> Glassy carbon. <i>Current density:</i> 1 mA cm ⁻² .	OP236 (<i>m/z</i> 237.1026)	Accurate mass (level 5): mass and spectral accuracy could not assign unequivocally a formula to the observed <i>m/z</i> .	Not reported previously.
		OP290 [2,4-diaminopyrimidin-5-yl)-(4-hydroxy-3,5-dimethoxyphenyl) methanone]	Probable structure (level 2b): based on spectral and mass accuracy, and comparative in-silico MS/MS fragmentation analysis.	Nitrifying bacteria in activated sludge [34].
		OP306 (α -OH-TRI)	Probable structure (level 2b): based on spectral and mass accuracy, experimental and literature MS/MS spectra.	Same as indicated for the three-compartment cell with stationary electrodes.
		OP322 (2OH-TRI) isomers	Tentative structures (level 3): based on spectral and mass accuracy, experimental and literature MS/MS spectra.	Direct photolysis and solar TiO ₂ photocatalysis [16], thermo-activated persulfate oxidation [19].
		OP324 (C ₁₄ H ₂₀ N ₄ O ₅)	Tentative structures (level 3): based on spectral and mass accuracy. Experimental and literature MS/MS spectra could not assign unambiguously one structure.	Nitrifying bacteria in activated sludge [22].
Thin-layer flow cell coupled online to HRMS	<i>Solution:</i> 0.1% FA in H ₂ O:ACN 1:1 <i>WE:</i> Boron-doped diamond. <i>Potential applied:</i> 1000 to 1500 vs. Pd/H ₂ .	OP306 (<i>m/z</i> 323.1372)	Accurate mass (level 5): mass and spectral accuracy could not assign unequivocally a formula to the observed <i>m/z</i> .	Same as indicated for the three-compartment cell with stationary electrodes.
		OP322 (2OH-TRI)	Tentative structures (level 3): based on spectral and mass accuracy, experimental and literature MS/MS spectra.	Same as indicated for the three-compartment cell with stationary electrodes.
		OP338 (<i>m/z</i> 339.1325)	Exact mass (level 5): mass and spectral accuracy could not assign unequivocally a formula to the observed <i>m/z</i> .	Photoelectro-Fenton with Pt anode [37].

WE: Working electrode.

4. Conclusions

Oxidation experiments with TRI using different electrochemical experiments (cyclic voltammetry, electrolysis, electro-assisted Fenton reaction and thin-layer flow cell coupled online to HRMS) generated several oxidation products previously reported in diverse biological processes such as bacterial and mammalian metabolism as well as in oxidation processes used for water treatment. Since many parameters intervened in the outcome of the experiments with each technique such as solution composition, pH, and electrode material, it is not possible to rank the techniques tested in terms of performance. Table 2 shows that the four setups differed especially in terms of selectivity in the production of oxidation products. Electrolysis using a glassy carbon electrode under $N_{2(g)}$ atmosphere was the most selective. This setup only generated OP306, identified as α -hydroxytrimethoprim (α -OH-TRI), as the major oxidation product. Electro-assisted Fenton oxidation and oxidation at a BDD anode in a thin-layer flow cell were less selective and generated an array of oxidation products. Among the most abundant were α -OH-TRI, 2OH-TRI and OP338, possibly a tri-hydroxylated derivative of TRI. The selectivity depends on the main oxidation mechanism involved in the techniques evaluated. In the three-compartment cell, the formation of α -OH-TRI is initiated by the transfer of one electron to the working electrode. In the electro-assisted Fenton oxidation in the one-compartment cell and in the oxidation at a BDD anode in the thin-layer flow cell, the $OH\bullet$ radical, a highly reactive oxidant with low selectivity towards organic compounds, plays a major role. Also, further studies with the thin-layer flow cell using different working electrodes, solution compositions, and pH values are needed, since the rapidity and simplicity of this technique makes it a quick and simple approach to study the fate of EOCs.

Finally, this study confirmed that electrochemical techniques are relevant not only to mimic the cytochrome P450 oxidation transformations of drugs, as has been suggested previously [10,13], but also to study the oxidation reactions of organic contaminants in wastewater treatment plants. The key role that redox reactions play in the environment make electrochemistry coupled to high resolution mass spectrometry a powerful technique to improve our understanding of the fate of EOCs in the environment.

Supplementary Materials: The following are available online at www.mdpi.com/2076-3298/5/1/18/s1, Figure S1. Simultaneous proposed mechanism of formation of α -OH-TRI (OP306). Since protons are generated at the anode during the electrolysis, TRI can be protonated in solution and then oxidized by initial loss of an electron from the trimethoxyl moiety rather than the diaminopyridinyl moiety. Figure S2. Survey view of the chromatogram obtained by UPLC-QTOFMS of a solution of TRI after 60 min of electrolysis at 1500 mV vs. Ag/Ag^+ using the setup described for the three-compartment electrochemical cell with stationary electrodes. The red circle indicates the peak corresponding to OP306 (m/z 307, α -hydroxytrimethoprim) and the blue square the peak corresponding to TRI (m/z 291). Peaks observed after 7 min correspond to compounds eluted at high organic percentage during the chromatographic separation. Signal threshold for the survey view was 1000 counts.

Acknowledgments: This research was funded by NSERC through a Discovery grant to Pedro A. Segura.

Author Contributions: Marc-André Lecours, Jean Lessard, Gessie M. Brisard and Pedro A. Segura conceived and designed the experiments; Marc-André Lecours performed the experiments and data analysis; Emmanuel Eysseric performed the spectral accuracy analysis; Viviane Yargeau contributed with access to Mass Frontier software; Jean Lessard provided mechanisms of oxidation of trimethoprim; Marc-André Lecours and Pedro A. Segura wrote the paper. All authors participated in the revision of the manuscript.

Conflicts of Interest: There are no conflicts of interest to declare.

References

1. Snyder, M.J. Cytochrome P450 enzymes in aquatic invertebrates: Recent advances and future directions. *Aquat. Toxicol.* **2000**, *48*, 529–547. [[CrossRef](#)]
2. Lohmann, W.; Karst, U. Biomimetic modeling of oxidative drug metabolism. *Anal. Bioanal. Chem.* **2008**, *391*, 79–96. [[CrossRef](#)] [[PubMed](#)]
3. Jahn, S.; Karst, U. Electrochemistry coupled to (liquid chromatography /) mass spectrometry—Current state and future perspectives. *J. Chromatogr. A* **2012**, *1259*, 16–49. [[CrossRef](#)] [[PubMed](#)]

4. Yan, Z.; Caldwell, G.W. Stable-isotope trapping and high-throughput screenings of reactive metabolites using the isotope MS signature. *Anal. Chem.* **2004**, *76*, 6835–6847. [[CrossRef](#)] [[PubMed](#)]
5. Glaze, W.H.; Kang, J.-W.; Chapin, D.H. The chemistry of water treatment processes involving ozone, hydrogen peroxide and ultraviolet radiation. *Ozone-Sci. Eng.* **1987**, *9*, 335–352. [[CrossRef](#)]
6. Ikehata, K.; Naghashkar, N.J.; El-Din, M.G. Degradation of aqueous pharmaceuticals by ozonation and advanced oxidation processes: A review. *Ozone-Sci. Eng.* **2006**, *28*, 353–414. [[CrossRef](#)]
7. Segura, P.A.; Saadi, K.; Clair, A.; Lecours, M.-A.; Yargeau, V. Application of XCMS online and toxicity bioassays to the study of transformation products of levofloxacin. *Water Sci. Technol.* **2015**, *72*, 1578–1587. [[CrossRef](#)] [[PubMed](#)]
8. Boxall, A.; Rudd, M.; Brooks, B.; Caldwell, D.; Choi, K.; Hickmann, S.; Innes, E.; Ostapyk, K.; Staveley, J.; Verslycke, T.; et al. Pharmaceuticals and Personal Care Products in the Environment: What are the Big Questions? *Environ. Health Perspect.* **2012**, *120*, 1221–1229. [[CrossRef](#)] [[PubMed](#)]
9. Bussy, U.; Chung-Davidson, Y.-W.; Li, K.; Li, W. Phase I and phase II reductive metabolism simulation of nitro aromatic xenobiotics with electrochemistry coupled with high resolution mass spectrometry. *Anal. Bioanal. Chem.* **2014**, *406*, 7253–7260. [[CrossRef](#)] [[PubMed](#)]
10. Johansson, T.; Weidolf, L.; Jurva, U. Mimicry of phase I drug metabolism—novel methods for metabolite characterization and synthesis. *Rapid Commun. Mass Spectrom.* **2007**, *21*, 2323–2331. [[CrossRef](#)] [[PubMed](#)]
11. Jurva, U.; Wikström, H.V.; Weidolf, L.; Bruins, A.P. Comparison between electrochemistry/mass spectrometry and cytochrome P450 catalyzed oxidation reactions. *Rapid Commun. Mass Spectrom.* **2003**, *17*, 800–810. [[CrossRef](#)] [[PubMed](#)]
12. Hoffmann, T.; Hofmann, D.; Klumpp, E.; Küppers, S. Electrochemistry-mass spectrometry for mechanistic studies and simulation of oxidation processes in the environment. *Anal. Bioanal. Chem.* **2011**, *399*, 1859–1868. [[CrossRef](#)] [[PubMed](#)]
13. Bussy, U.; Boujtita, M. Advances in the electrochemical simulation of oxidation reactions mediated by cytochrome P450. *Chem. Res. Toxicol.* **2014**, *27*, 1652–1668. [[CrossRef](#)] [[PubMed](#)]
14. Seiwert, B.; Golan-Rozen, N.; Weidauer, C.; Riemenschneider, C.; Chefetz, B.; Hadar, Y.; Reemtsma, T. Electrochemistry Combined with LC–HRMS: Elucidating Transformation Products of the Recalcitrant Pharmaceutical Compound Carbamazepine Generated by the White-Rot Fungus *Pleurotus ostreatus*. *Environ. Sci. Technol.* **2015**, *49*, 12342–12350. [[CrossRef](#)] [[PubMed](#)]
15. Segura, P.A.; Takada, H.; Correa, J.A.; El Saadi, K.; Koike, T.; Onwona-Agyeman, S.; Ofosu-Anim, J.; Sabi, E.B.; Wasonga, O.V.; Mghalu, J.M.; et al. Global occurrence of anti-infectives in contaminated surface waters: Impact of income inequality between countries. *Environ. Int.* **2015**, *80*, 89–97. [[CrossRef](#)] [[PubMed](#)]
16. Sirtori, C.; Agüera, A.; Gernjak, W.; Malato, S. Effect of water-matrix composition on Trimethoprim solar photodegradation kinetics and pathways. *Water Res.* **2010**, *44*, 2735–2744. [[CrossRef](#)] [[PubMed](#)]
17. Kuang, J.; Huang, J.; Wang, B.; Cao, Q.; Deng, S.; Yu, G. Ozonation of trimethoprim in aqueous solution: Identification of reaction products and their toxicity. *Water Res.* **2013**, *47*, 2863–2872. [[CrossRef](#)] [[PubMed](#)]
18. Hu, L.; Stemig, A.M.; Wammer, K.H.; Strathmann, T.J. Oxidation of antibiotics during water treatment with potassium permanganate: Reaction pathways and deactivation. *Environ. Sci. Technol.* **2011**, *45*, 3635–3642. [[CrossRef](#)] [[PubMed](#)]
19. Ji, Y.; Xie, W.; Fan, Y.; Shi, Y.; Kong, D.; Lu, J. Degradation of trimethoprim by thermo-activated persulfate oxidation: Reaction kinetics and transformation mechanisms. *Chem. Eng. J.* **2016**, *286*, 16–24. [[CrossRef](#)]
20. Michael, I.; Hapeshi, E.; Osorio, V.; Perez, S.; Petrovic, M.; Zapata, A.; Malato, S.; Barceló, D.; Fatta-Kassinos, D. Solar photocatalytic treatment of trimethoprim in four environmental matrices at a pilot scale: Transformation products and ecotoxicity evaluation. *Sci. Total Environ.* **2012**, *430*, 167–173. [[CrossRef](#)] [[PubMed](#)]
21. Radjenović, J.; Godehardt, M.; Hein, A.; Farré, M.; Jekel, M.; Barceló, D. Evidencing generation of persistent ozonation products of antibiotics roxithromycin and trimethoprim. *Environ. Sci. Technol.* **2009**, *43*, 6808–6815. [[CrossRef](#)] [[PubMed](#)]
22. Eichhorn, P.; Ferguson, P.L.; Pérez, S.; Aga, D.S. Application of ion trap-MS with H/D exchange and QqTOF-MS in the identification of microbial degradates of trimethoprim in nitrifying activated sludge. *Anal. Chem.* **2005**, *77*, 4176–4184. [[CrossRef](#)] [[PubMed](#)]

23. Zhang, Z.; He, L.; Lu, L.; Liu, Y.; Dong, G.; Miao, J.; Luo, P. Characterization and quantification of the chemical compositions of *Scutellariae Barbatae* herba and differentiation from its substitute by combining UHPLC–PDA–QTOF–MS/MS with UHPLC–MS/MS. *J. Pharm. Biomed. Anal.* **2015**, *109*, 62–66. [[CrossRef](#)] [[PubMed](#)]
24. Nouri-Nigjeh, E.; Permentier, H.P.; Bischoff, R.; Bruins, A.P. Lidocaine oxidation by electrogenerated reactive oxygen species in the light of oxidative drug metabolism. *Anal. Chem.* **2010**, *82*, 7625–7633. [[CrossRef](#)] [[PubMed](#)]
25. Nouri-Nigjeh, E.; Permentier, H.P.; Bischoff, R.; Bruins, A.P. Electrochemical oxidation by square-wave potential pulses in the imitation of oxidative drug metabolism. *Anal. Chem.* **2011**, *83*, 5519–5525. [[CrossRef](#)] [[PubMed](#)]
26. Oloman, C.; Watkinson, A. Hydrogen peroxide production in trickle-bed electrochemical reactors. *J. Appl. Electrochem.* **1979**, *9*, 117–123. [[CrossRef](#)]
27. Dodd, M.C.; Buffle, M.-O.; Von Gunten, U. Oxidation of antibacterial molecules by aqueous ozone: Moiety-specific reaction kinetics and application to ozone-based wastewater treatment. *Environ. Sci. Technol.* **2006**, *40*, 1969–1977. [[CrossRef](#)] [[PubMed](#)]
28. Antec. *m-Prepcell User Manual (204.0010, 5th ed.)*; Antec: Zoeterwoude, The Netherlands, 2013; p. 45.
29. Schymanski, E.L.; Jeon, J.; Gulde, R.; Fenner, K.; Ruff, M.; Singer, H.P.; Hollender, J. Identifying small molecules via high resolution mass spectrometry: Communicating confidence. *Environ. Sci. Technol.* **2014**, *48*, 2097–2098. [[CrossRef](#)] [[PubMed](#)]
30. Eysseric, E.; Bellerose, X.; Lavoie, J.-M.; Segura, P.A. Post-column hydrogen-deuterium exchange technique to assist in the identification of small organic molecules by mass spectrometry. *Can. J. Chem.* **2016**, *94*, 781–787. [[CrossRef](#)]
31. Wang, Y.; Gu, M. The concept of spectral accuracy for MS. *Anal. Chem.* **2010**, *82*, 7055–7062. [[CrossRef](#)] [[PubMed](#)]
32. Meshi, T.; Sato, Y. Studies on sulfamethoxazole/trimethoprim. Absorption, distribution, excretion and metabolism of trimethoprim in rat. *Chem. Pharm. Bull.* **1972**, *20*, 2079–2090. [[CrossRef](#)] [[PubMed](#)]
33. Liu, W.-T.; Li, K.-C. Application of reutilization technology to calcium fluoride sludge from semiconductor manufacturers. *J. Air Waste Manag. Assoc.* **2011**, *61*, 85–91. [[CrossRef](#)] [[PubMed](#)]
34. Jewell, K.S.; Castronovo, S.; Wick, A.; Falás, P.; Joss, A.; Ternes, T.A. New insights into the transformation of trimethoprim during biological wastewater treatment. *Water Res.* **2016**, *88*, 550–557. [[CrossRef](#)] [[PubMed](#)]
35. Baumann, A.; Lohmann, W.; Jahn, S.; Karst, U. On-Line Electrochemistry/Electrospray Ionization Mass Spectrometry (EC/ESI-MS) for the Generation and Identification of Nucleotide Oxidation Products. *Electroanalysis* **2010**, *22*, 286–292. [[CrossRef](#)]
36. Marselli, B.; Garcia-Gomez, J.; Michaud, P.-A.; Rodrigo, M.; Comninellis, C. Electrogeneration of hydroxyl radicals on boron-doped diamond electrodes. *J. Electrochem. Soc.* **2003**, *150*, D79–D83. [[CrossRef](#)]
37. Moreira, F.C.; Garcia-Segura, S.; Boaventura, R.A.; Brillas, E.; Vilar, V.J. Degradation of the antibiotic trimethoprim by electrochemical advanced oxidation processes using a carbon-PTFE air-diffusion cathode and a boron-doped diamond or platinum anode. *Appl. Catal. B Environ.* **2014**, *160*, 492–505. [[CrossRef](#)]
38. Gattrell, M.; Kirk, D. A study of electrode passivation during aqueous phenol electrolysis. *J. Electrochem. Soc.* **1993**, *140*, 903–911. [[CrossRef](#)]
39. Jahn, S.; Faber, H.; Zazzeroni, R.; Karst, U. Electrochemistry/mass spectrometry as a tool in the investigation of the potent skin sensitizer p-phenylenediamine and its reactivity toward nucleophiles. *Rapid Commun. Mass Spectrom.* **2012**, *26*, 1453–1464. [[CrossRef](#)] [[PubMed](#)]

